Experimental and analytical investigation of thermal coating effectiveness for 3 m³ LPG tanks engulfed by fire

Gabriele Landucci [a], Menso Molag [b], Johan Reinders [b], Valerio Cozzani [c],*

[a] CONPRICI – Dipartimento di Ingegneria Chimica, Chimica Industriale e Scienza dei Materiali, Università degli Studi di Pisa, via Diotisalvi n.2, 56126 Pisa, Italy
[b] Nederlandse Organisatie voor toegepast-natuurwetenschappelijk onderzoek TNO, Laan van Westenenk 501, P.O. Box 342, 7300 AH Apeldoorn, The Netherlands
[c] CONPRICI – Dipartimento di Ingegneria Chimica, Mineraria e delle Tecnologie Ambientali, Alma Mater Studiorum, Università di Bologna,
via Terracini n.28, 40131 Bologna, Italy

ARTICLE INFO

ABSTRACT

Two large-scale diesel pool fire engulfment tests were carried out on LPG tanks protected with intumescing materials to test the effectiveness of thermal coatings in the prevention of hot BLEVE accidental scenarios in the road and rail transport of LPG. A specific test protocol was defined to enhance reproducibility of experimental tests. The geometrical characteristics of the test tanks were selected in order to obtain shell stresses similar to those present in full-size road tankers complying to ADR standards. In order to better understand the stress distribution on the vessel and to identify underlying complicating phenomena, a finite element model was also developed to better analyze the experimental data. A non-homogeneous and time-dependent effectiveness of the fire protection given by the intumescing coating was evidenced both by finite element simulations and by the analysis of the coating after the tests. The results of the fire tests pointed out that the coating assured an effective protection of the tanks, consistently increasing the expected time to failure. The data obtained suggest that the introduction of fire protection coatings may be a viable route to improve the safety of the LPG distribution chain.

© 2008 Elsevier B.V. All rights reserved.

1. Introduction

Several studies on the risks associated with the production, transport and use chain of ammonia, chlorine and liquefied petroleum gas (LPG) in the Netherlands were carried out by TNO in the period 2002–2005 [1]. In these studies, a relevant number of sites were identified where the Dutch external safety criteria for societal and location specific risk (also named individual risk in some literature sources) was not complied. In particular, the results of these studies indicated that, despite existing safety measures, 550 over of a total of 2100 LPG filling stations exceeded the admissible value for societal risk. The main cause of these results was in the potential consequences of accidental scenarios due to fired boiling liquid expanding vapour explosions (BLEVEs) of LPG road tankers during loading/unloading operations. Data on several fire tests carried out at different scales [2–4] pointed out that engulfed LPG tanks with no fire protection may withstand pool fire engulfment conditions for time lapses typically comprised between 10 and 25 min, depending on fire and tank characteristics, before collapsing and causing a hot BLEVE. This result was confirmed also

by model data reported for the time to BLEVE in the case of full engulfment calculated for LPG tanks [5–7]. Such a time lapse was considered not sufficient to assure an effective mitigation by external fire brigades. A realistic evaluation of the time required for effective mitigation by the fire brigades, based on actual data available from past accidents in the Netherlands, evidenced that a time lapse of 75 min is required to allow an effective protection or prevention of BLEVE by active measures upon the arrival of the fire brigades [8].

Thus, although not required by the current European agreement concerning the international carriage of dangerous goods by road (ADR) agreements for road transport of LPG [9], the adoption of passive protections was considered to increase the time required for a hot BLEVE and/or to prevent it. The application of a heat resistant coating on the outer tank surface and of a pressure relief valve (PRV) were considered. Although these are well-known protection systems, scarce data are available in the open literature concerning the performance of LPG tanks protected with intumescing coatings [10].

Therefore, in order to investigate the coupled protective action of PRV and thermal insulating coating a test protocol was defined. The protocol had the purpose to test the vessel integrity after a time sufficient for an effective mitigation. Two tests were thus carried out using coated tanks engulfed by a diesel pool fire. In the following,

* Corresponding author. Tel.: +39 051 2090240; fax: +39 051 2090247.
E-mail address: valerio.cozzani@unibo.it (V. Cozzani).

ADR	European agreement concerning the international carriage of dangerous goods by road
B	stiffness matrix
b	elements of the stiffness matrix
BLEVE	boiling liquid expanding vapour explosions
c	heat capacity
D	tank diameter
FEM	finite element modeling
F_M	mechanical forces vector
F_T	initial forces vector
g	gravity acceleration
h	heat transfer coefficient between the tank wall and the inner fluid
i	definition of the nodal force
j	definition of the nodal strain
k	thermal conductivity
LPG	liquefied petroleum gas
n	time step
p	internal pressure
PRV	pressure relief valve
Q_{conv}	convective heat flux from the steel wall to the inner fluid
Q_{rad}	heat load due to the flame impingement on coating surface
r	radial coordinate
RID	European agreement concerning the international carriage of dangerous goods by rail
S	mechanical surface loads among the tank
t	time
T	temperature
T_B	bulk fluid temperature
u	displacement vector
z	axial coordinate

Greek letters

α	thermal dilatation coefficient
ε_T	thermal imposed strain
ϕ	angular coordinate
ρ	material density
ρ_l	liquid density

the results of the experimental tests were described and analyzed. In order to better understand the stress distribution on the vessel and to identify underlying complicating phenomena, a finite element model was also developed to interpret the experimental data.

2. Experimental analysis

2.1. General layout

Since no standard experimental protocol exists to test heat resistant coatings for road or rail tankers, the protocol used to test LPG tanks used for fuel supply in cars was taken as a blue-print to set-up the test criteria [11,12]. On the basis of the above discussion, a duration of at least 75 min was required for the experimental tests. The following set of test criteria were thus defined:

1. Within 5 min after the remote ignition of the diesel pool fire, the average flame temperature should be at least 590 °C. This temperature should be kept constant throughout the remainder
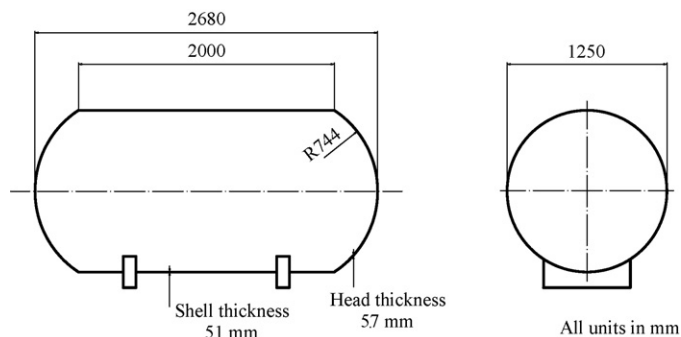

Fig. 1. Geometrical characteristics of the test tanks (all numerical values are in mm).

of the test period in at least 50% of the total local measurement positions
2. The tank should be fully engulfed in flames for at least 75 min
3. The tank should contain liquid LPG for at least 75 min
4. LPG may only leave the tank through the PRV
5. The opening pressure of the PRV should be equal to its set-point value

To assess these criteria the pressure inside the tank and the temperature of the tank wall were monitored during the test. Also the temperatures of the liquid and vapour phases inside the tank and of the flame outside the tank were measured.
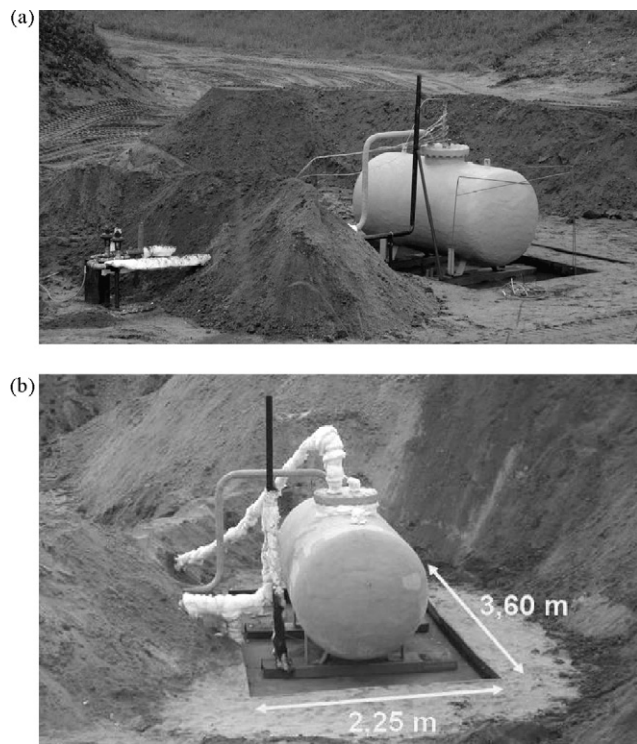
2.2. Test tanks

3 m³ propane tanks having a diameter of 1250 mm and an overall length of 2680 mm realized according to the European ADR/RID standard certification [13] were used in the test. The diameter of the trial tanks was chosen in order to be close to that of tanks used for road transport of LPG. In particular it corresponded to the 50% of the nominal diameter of a standard European 60 m³ road tanker and to 40% of a 100 m³ rail tanker [8]. Further geometrical details of the trial tanks are reported in Fig. 1 and in Table 1.

The tanks were built using WST E 355N DIN 17102 steel, having a minimum ultimate tensile strength of 490 MPa at 40 °C. This material is nearly identical to the ASME equivalent A 516 Gr. 70. The tank was equipped with a standard DN500-EN28043 manhole, in order to connect the thermocouples and the pressure transducer inside of the tank.

The design gauge pressure was 1.46 MPa at 40 °C. The design pressure was set considering the theoretical maximum allowable stress on the tank and considering the typical design condition of large-scale tanks for LPG transportation. In particular, the average design gauge pressure of LPG road tankers used in the Netherlands is of about 1.83 MPa [1,8]. Since the aim of the test was to obtain

Table 1
Characteristics of test tanks

Item	Specification
Supplier/tank code	ABR GmbH, no. 07184 and 07185
Shape	Cylinder
Material	WSt.E 355N DIN 17102
Diameter (m)	1.25
Length (m)	2.68 (end-to-end)
External surface area (m²)	9.3
Minimum wall thickness – shell (mm)	5.1
Minimum wall thickness – (end caps) (mm)	5.7
Capacity (m³)	2.96
Design gauge pressure (MPa)	1.46 at 40 °C
Burst pressure (MPa) at 40 °C	4.00
Year of construction	1993

(a)

(b)

3,60 m

2,25 m

Fig. 2. The experimental set-up: (a) overview of the tank, the sand wall and the PRV (on the left side); (b) bonfire detail (tray sizes are in m).

significant data to interpret the behaviour of larger scale road tankers, the design pressure of the test tank was reduced in order to obtain the same value of the circumferential stress even in the presence of a different diameter/thickness ratio.

2.3. Tank passive fire protections

Originally the test tanks were equipped with a spring operated PRV. After some preliminary trials, this was substituted with an electronically controlled pressure relief valve, to avoid the influence of temperature on the opening pressure (due to the spring softening) and to increase the reliability of the system [14]. Since the opening pressure decreases with temperature, this choice assured conservative results to be obtained. The PRV had a set point of 1.46 MPa for the opening gauge pressure and of 1.3 MPa for the closing gauge pressure.

To avoid damage due to the fire, the PRV was positioned outside the fire and the relief line was protected by thermal insulation material (see Fig. 2a). The vented gas was returned to a position just above the tank, to simulate the vent from an actual PRV. This also assured the vented gas to be ignited. More details on the PRV are reported in Table 2.

A filling level of 80% (2.4 m³ or 1200 kg) was chosen for the first experiment (named as test A in the following), to assure that liq-

Table 2
Characteristics of the pressure relief valve

Item	Specification
Supplier/code	Badger meter Europa GmBH Serial number G11684 Mod. no. 1064GCN67CV0S60PST
Opening gauge pressure (MPa)	1.46
Closing gauge pressure (MPa)	1.30 (90% of opening pressure)
Nominal diameter (mm)	1¼ in. (32 mm)

Table 3
Characteristics and average physical properties of the thermal protection coating in the temperature field of interest provided by the supplier

Material	Chartek® 7
Supplier	International Paint®
Average nominal thickness (mm)	10
Heat capacity (J/kg K)	1172

uid LPG would be present in the tank for at least 75 min after the beginning of the test. Due to limited venting from the PRV, a lower liquid level was thus chosen (50% filling level) for a second test (test B), resulting in a larger portion of the vessel walls in contact with the vapour, experiencing more severe heat loading conditions [3]. Grade A (EN27941) type LPG (approximately 70% propane and 30% butane) was used to fill the vessel.

The test tanks were protected with a heat resistant coating. An epoxy intumescent material was selected. Table 3 reports the average physical properties provided by the supplier of the coating. During the fire exposure this type of coating expands as a result of the massive heating. A "foaming" effect which increases the insulating properties of the material is caused by the decomposition of the volatile products and by the charring process [15]. This also causes the material to be slowly burned by the flames, in particular on the outer surface. The application of several layers of material is thus necessary to assure a sufficient duration of the fire protection. The presence of unreacted coating material in the layers near to the vessel wall thus indicates a residual capacity of the fire protection.

On the basis of the previous considerations and according to the suggestions of the provider, a coating thickness of 10 ± 1.5 mm was selected. In particular, in order to obtain a more uniform protective effect, a first layer of 5 mm was applied smearing the epoxy paste on the tank surface. A reinforcing carbon fiber mesh was then applied and a second 5 mm layer of intumescing paste was applied. Fig. 3a shows the application of the heat resistant coating. A specific testing probe, having an accuracy of 0.05 mm, was used to verify the thickness of the coating in different positions, as shown in Fig. 3b.

2.4. Experimental procedure

A diesel pool fire was used to reproduce on a small scale full engulfment conditions with flames having a minimum temperature of 590 °C for at least 75 min. Since wind had a relevant effect on the results of the first test (test A), a sand wall was built in order to limit the effect of the wind on the experimental results obtained in the second test (test B).

Fig. 2b shows the details of the system. A rectangular tray measuring 3.60 m × 2.25 m was filled with approximately 0.9 m³ of diesel fuel (UN 1202). Additional fuel was pumped into the tray during the experiment from a buffer vessel having a volume of 2.5 m³. At the beginning of the experiments, 80 L of gasoline were added to the diesel fuel to aid the ignition. The fuel was ignited firing four small bags filled with gun-powder placed at the four corners of the fuel tray.

The test tanks were equipped with 18 type K Chromel/Alumel thermocouples, assuring temperature reading with an average error of ±1 °C between 0 and 350 °C, and with a static pressure transducer, having an average error of ±0.02 bar. During the experimental runs, temperature and pressure data were recorded every 5 s.

A simplified sketch of the positions of the thermocouples is reported in Fig. 4. A total of eight thermocouples were applied for inner wall temperatures measurement. Two other thermocouples were positioned 50 mm below the top of the tank and 50 mm above the bottom of the tank, in order to measure respectively the

(a)

(b)
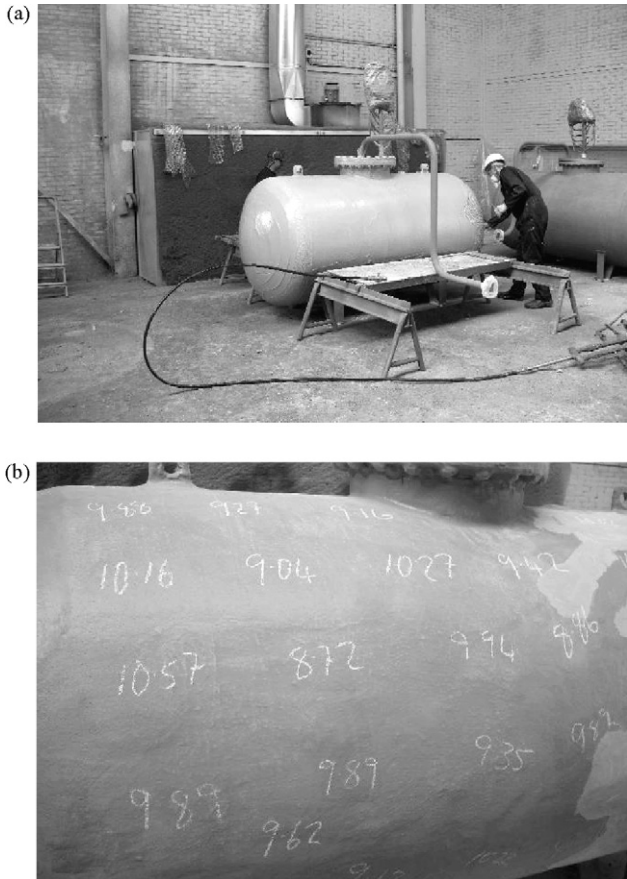
Fig. 3. (a) Application of the heat resistant coating to a test tank. (b) Side view of tank used for test A showing the measured values of the coating thickness (in mm).

liquid and vapour LPG bulk temperatures. Other eight thermocouples were applied outside the tank. Two of them were positioned just below the test tank, near the tank supports. The other six were positioned outside the tank halfway, in order to assess the effectiveness of the fire engulfment during the experiment (Fig. 4).

The temperature of the PRV was also monitored for safety reasons.

2.5. Result and discussion

Two experimental tests (test A and test B) were performed using identical 3 m³ tanks having the characteristics discussed in Section 2. Test A was carried out before the realization of the protective sand wall shown in Fig. 2. In this test, strong wind effects reduced the flame temperature and caused only a partial impingement of the test tank (Fig. 5a). The requirements of the experimental protocol were thus not satisfied.

Test B, carried out after the realization of the protective sand wall fulfilled all the conditions required by the above defined experimental protocol. The tank was uniformly engulfed in the flames for the entire duration of the experiment, as shown in Fig. 5b.

Even if in test A the requirements of the experimental protocol were not fulfilled, useful data were obtained on the effect of wind on wall temperatures during pool fire engulfment. These data are particularly significant if compared to those obtained in test B, where these effects were limited. Thus, the results of both tests are presented and discussed in the following.

2.5.1. Test A

Test A had a total duration of 98 min. The test tank was initially filled with 2.4 m³ of LPG (80% filling level). In Fig. 6b, the bulk temperatures of both gas and liquid phases are reported. During the test, the PRV opened 5 times, as shown in Fig. 6a. As evident from the figure, the vapour temperatures increased to 103 °C due to the tank heating, and rapidly decreased to 60 °C after the PRV opening. The liquid temperature reached a maximum value of 65 °C, decreasing to 60 °C after the PRV opening. After the fifth opening of the PRV the experiment was terminated by setting the valve closing pressure to 0.1 MPa. This caused the LPG still present in the tank (approximately 25% of initial content) to vent.

The temperatures of the vessel wall in contact with the vapour phase (T3 and T7) are reported in Fig. 7. As shown in the figure, significant differences are present. While the left side of the vessel (T3) has temperatures corresponding to full engulfment conditions (215 °C after 75 min and a maximum value of 227 °C at the test
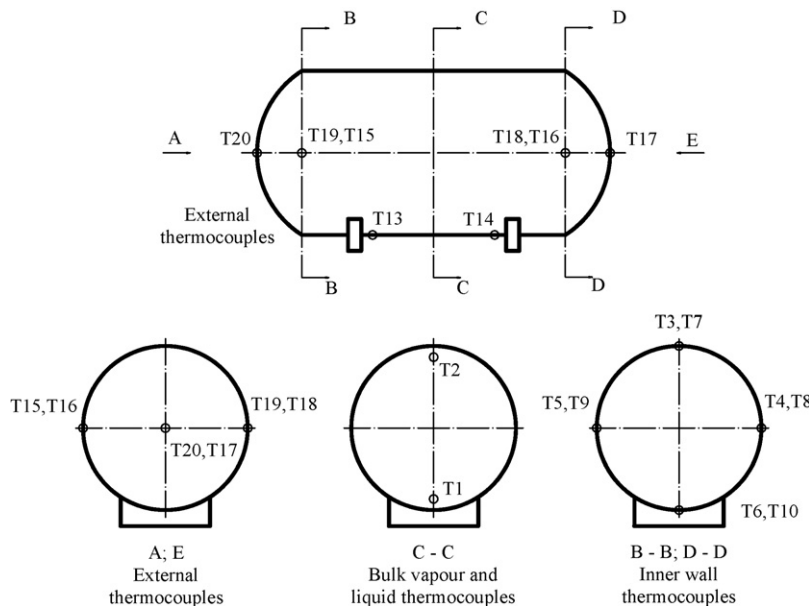
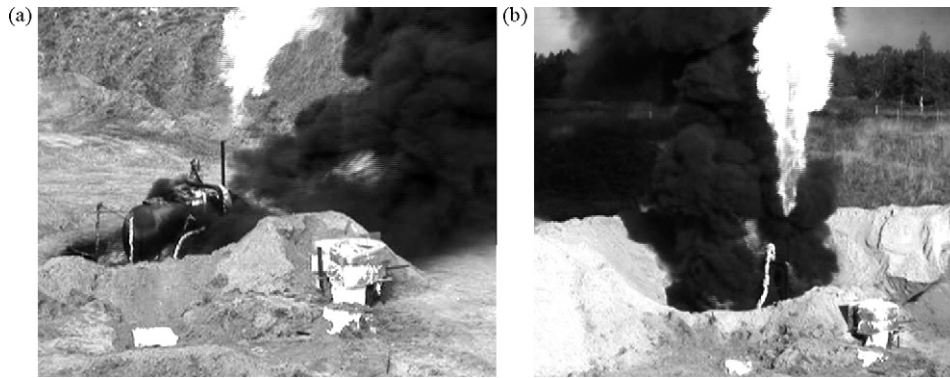**Fig. 4.** Position of thermocouples on the test tanks.

Fig. 5. (a) Test A: a non-uniform engulfment in flames is observed, caused by the wind. (b) Test B: the sand wall limited the effect of wind, allowing a more uniform fire engulfment.
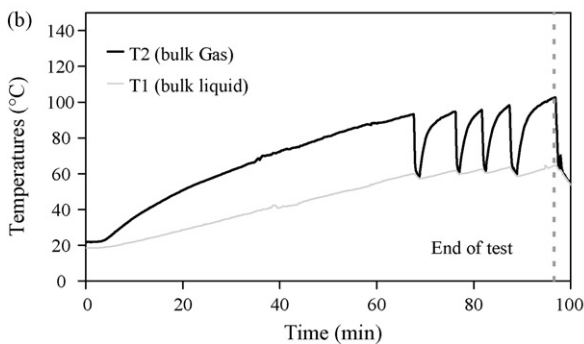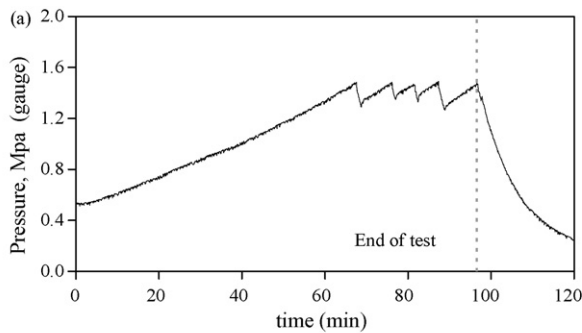

Fig. 6. Tank pressure (a) and bulk fluid temperatures (b) during test A.

Fig. 7. Tank wall temperatures during test A.

end after 98 min), the right side thermocouple signal (T7) shows that lower wall temperatures are present (99 °C after 75 min and a maximum value of 109 °C at the test end after 98 min). This was possibly caused by wind effects. As a matter of fact, visual observations and flame temperature measurements (see Table 4) showed that frequently during the test, the tank was not fully engulfed in the flames, and the average flame temperature on the upwind side of the tank fell below the required minimum of 590 °C in five of the eight measurement spots several times after 5 min from the beginning of the test.

The more uniform liquid bulk temperatures recorded (see the T1 signal in Fig. 7) are possibly due to the violent bubbling of the liquid, and to the liquid entrainment following the PRV opening [16–18]. Temperature measurements in different positions of the wall in contact with the liquid showed the same qualitative behaviour before the PRV opening, with the temperature rising up to 66 °C. After the PRV opening, temperatures measured in the bottom part of the tank (see Fig. 7, thermocouples T6 and T10) were higher than the others (about 5 °C). This may have been caused by wind effects, that caused lower heat loads on the upper part of the tank, exposed to the wind.

The results of this test confirmed the strong importance of wind effects on the thermal effects deriving from fire engulfment, also experienced in previous experimental studies [8,14]. As a matter of fact, the wind effects caused a difference of more than 100 °C in maximum wall temperatures and significantly lower heat loads on the upwind wall of the tank. Moreover, the test confirmed that, as expected, the higher temperatures are experienced in the wall sections in contact with the vapour.

2.5.2. Test B

Test A provided useful information both on the effectiveness of the experimental set-up and on wind effects. However, the non-uniform fire conditions caused by the wind and the low wall
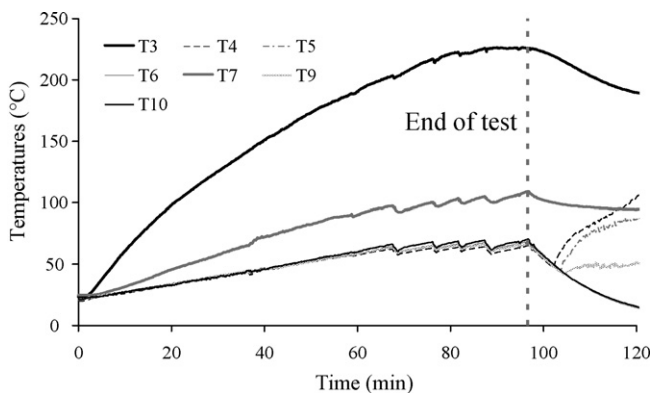
Table 4
Maximum, average and minimum flame temperatures in test A

ID thermocouple	Flame temperatures (°C)		
	Maximum value	Minimum value after 5 min	Average value
T13	928	49	343
T14	1137	649	827
T15	641	88	176
T16	817	241	439
T17	1007	549	720
T18	1313	565	983
T19	727	195	312
T20	356	66	125

(a) Pressure graph

(b) Temperature graph
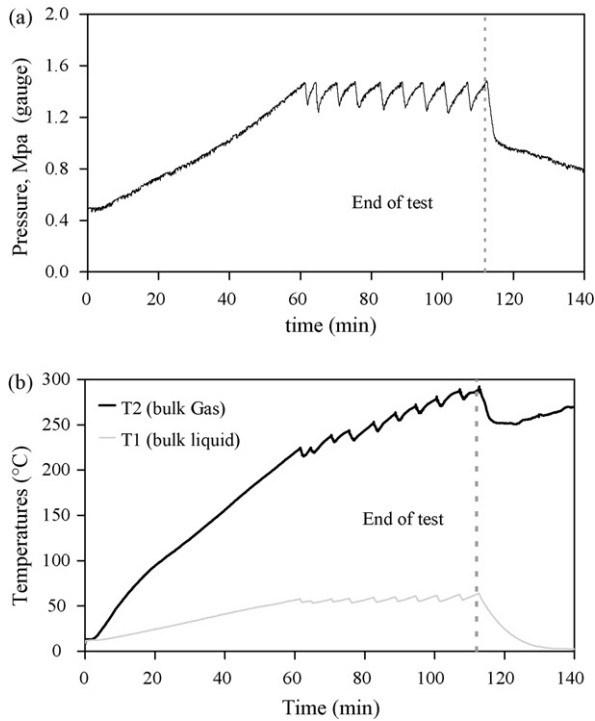
Fig. 8. Tank pressure (a) and bulk fluid temperatures (b) during test B.

Fig. 9. Tank wall temperatures during test B.

temperatures actually mitigated the possible effect of a full fire engulfment in the absence of wind. Thus, a further test (test B) was carried out following the same experimental protocol of test A, but applying some modifications to the experimental set-up. In order to limit the previously mentioned wind effects, a sand wall was built. A lower filling level (50%, corresponding to 1.5 m^3 of LPG) was used, resulting in a larger portion of the vessel walls in contact with the vapour and thus experiencing more severe heat loading conditions, as evidenced in test A.

Test B lasted 112 min. Fig. 8a reports the internal tank pressure recorded during the test. The figure shows that after an initial heat-up period, the PRV opened 9 times before the end of the experiment, when the PRV was manually opened venting to atmosphere 0.8 m^3 of LPG still present in the tank. The limitation of wind effects by the sand wall resulted in more severe fire conditions, and a uniform fire impingement on the tank was realized. After 25 s the flame temperature reached the minimum required value of 590 °C. During the remainder of the experiment, the average flame temperature was over this value in seven of the total eight measurement spots for the flame temperature. Thus the test successfully fulfilled all protocol requirements, as shown in Table 5.

Table 5
Maximum, average and minimum flame temperatures in test B

ID thermocouple	Flame temperatures (°C)		
	Maximum value	Minimum value after 5 min	Average value
T13	1006	592	831
T14	1034	651	858
T15	1058	342	783
T16	1191	592	966
T17	1027	373	646
T18	1184	285	696
T19	1054	284	569
T20	971	189	447
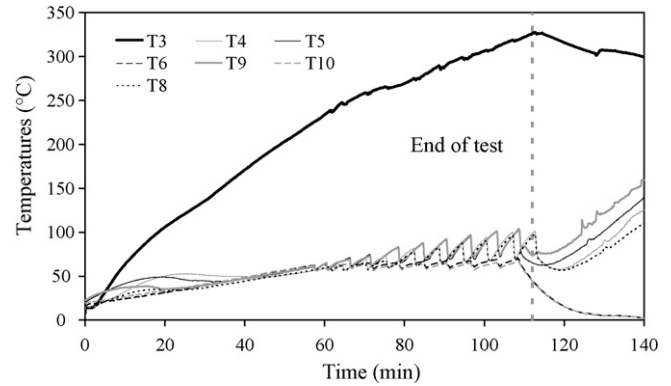
Fig. 8b shows the bulk temperatures of both the gas and the liquid phase during the test. The vapour temperatures increased to 292 °C until PRV opening. After the opening of the PRV, the temperature decreased, but remained higher than in test A. This was probably due to the effect of the lower filling level, that avoided liquid entrainment effects on the thermocouple. Maximum vapour temperatures were almost three times higher than in test A, due to the higher heat loads. On the other hand, the behaviour of liquid temperature is almost the same of that recorded for test A, with a maximum temperature of 65 °C that decreased to 60 °C after PRV opening. This is due to the action of the electronic PRV, that maintained the same range of internal tank pressures in both tests.

Recorded wall temperatures are reported in Fig. 9. As evident from the figure, three quite different zones may be identified on the vessel shell: (i) the upper zone in contact with the vapour phase; (ii) the middle zone in contact with the interface between vapour and liquid phases; and (iii) the lower zone in contact with the liquid phase. The upper part (T3 in Fig. 9) is characterized by the higher temperatures, that reach 266 °C after 75 min and a maximum temperature of 328 °C at the end of the test. In the bottom zone (T6 and T10 in Fig. 9), in contact with the liquid phase, the same behaviour obtained in test A was recorded: wall temperatures uniformly increase up to 66 °C and then begin to oscillate between 65 and 60 °C due to the PRV opening.

In the middle zone of the vessel (T4, T5, T8 and T9 in Fig. 9), the thermocouples are in contact with the liquid–vapour interface. In this zone, initially the temperatures are similar to that of the bottom zone. However, after the first PRV opening the temperature increases more rapidly and shows wider oscillations than in the bottom zone. Possibly, in the second part of the test, liquid level decrease due to venting caused these thermocouples to be in contact with gas when the PRV is closed, while during vent opening violent boiling and liquid expansion caused the wall temperatures to decrease to values very close to those of the liquid. Similar behaviours of wall temperatures at liquid interfaces were experienced in previous studies [3].

A final remark is that the wall temperature values reported in Fig. 9 evidence the effectiveness of the thermal coating, that allowed the tank to resist to pool fire full engulfment conditions for more than the minimum response time of 75 min defined by the test protocol. This was confirmed also by the analysis of the coating carried out after the test. Coating thicknesses were measured with the technique discussed in Section 2.3 in 60 different positions of the vessel shell at the end of the test. The results evidenced that the coating thickness after the test ranged between 10 and 48 mm. Higher thicknesses were present in the upper zone of the vessel shell. The average expansion factor due to the intumescing effect resulted of 2.5. An average coating thickness of 25 mm
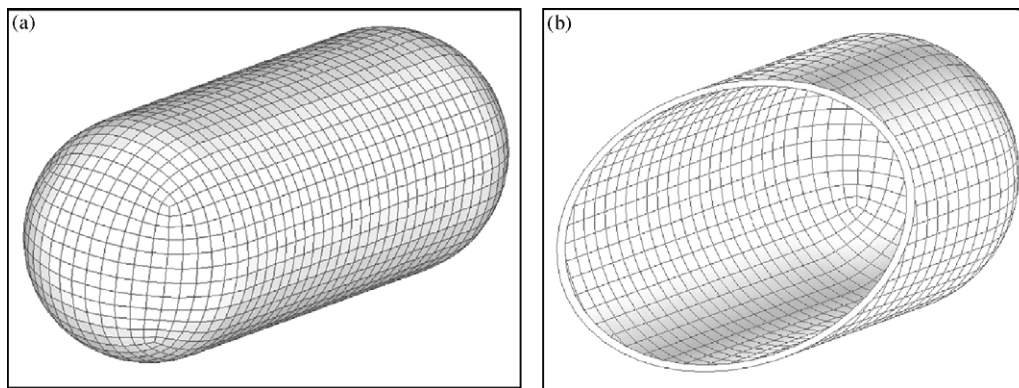
Fig. 10. Detail of the mesh used for finite element modeling. (a) Overview; (b) tank section.

may be thus considered sufficient to provide adequate protection from the thermal load in order to satisfy the conditions required by the experimental protocol.

3. Numerical analysis

3.1. Modeling experimental results

In order to better understand the thermal and mechanical behaviour of the tank structure during the test, a simplified modeling of the shell temperature and stresses was undertaken. The model was also aimed to understand the influence on test results of some complicating phenomena, e.g. as coating consumption due to charring, not considered in the approach developed. Finite element modeling was used to obtain detailed temperature and stress maps of the vessel shell. The finite element model (FEM) was implemented using the ANSYS software. Detailed simulations of the radiation mode, of the wall temperature and of the stress over the vessel shell were performed.

The first step in the simulations was the detailed calculation of the temperatures on the vessel shell as a function of time and of external thermal loads. The tank was modeled as a cylindrical body with spherical heads. The geometry was schematized using an uniform brick mesh for the calculations, having more than 6192 cells (see details in Fig. 10). An insulating coating having constant properties and constant thickness was considered in the model. The final average coating thickness measured after test B was used

Table 6
Parameters used in the FEM simulations

| Item	Physical property	Value	Unit (SI)
Steel	Thermal conductivity	50	W/m K
	Heat capacity	460	J/kg K
	Surface emissivity	0.4	–
	Density	7850	kg/m³
	Thermal dilatation coefficient	11.5	ppm/K
	Poisson's ratio	0.3	–
	Elastic modulus	201.5	GPa
Insulating material	Thermal conductivity	0.066	W/m K
	Heat capacity	1172	J/kg K
	Surface emissivity	0.9	–
	Density	1000	kg/m³
	Thermal dilatation coefficient	11.5	ppm/K
	Poisson's ratio	0.3	–
	Elastic modulus	1	GPa
Fire test parameters	Pool fire radiation intensity	110000	W/m²
	Test time	6720	s
	Time step	20	s
	Initial temperature conditions	285	K
Bulk liquid parameters	Density	585	kg/m³
	Temperature	338	K
	Heat transfer coefficient	400	W/m² K
Bulk vapour parameters	Temperature	560	K
	Heat transfer coefficient	6	W/m² K
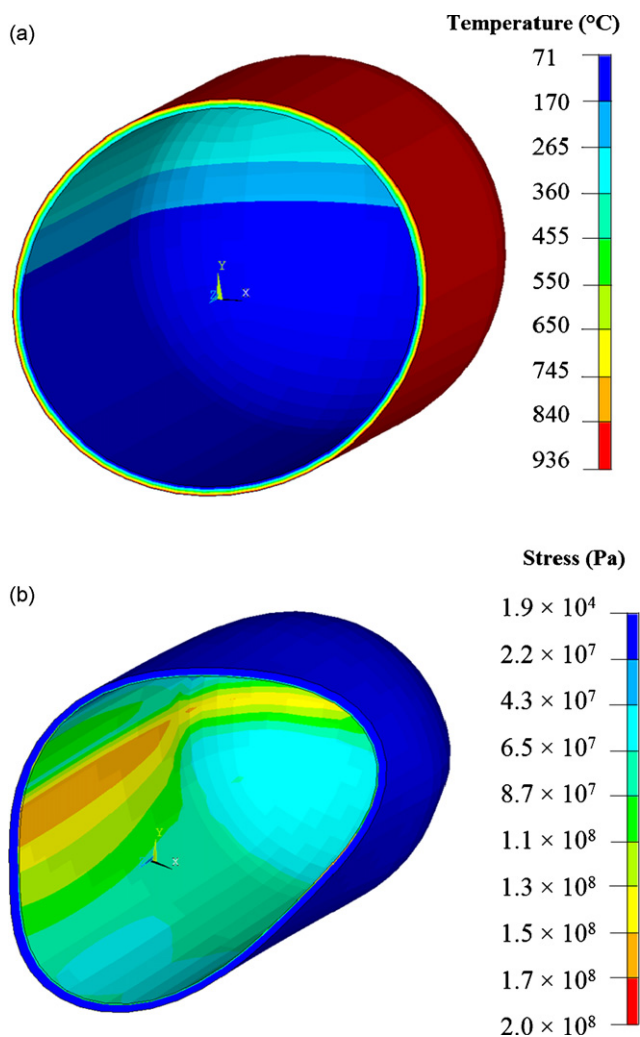
Fig. 11. Results of FEM simulations: (a) temperature map (°C) obtained for test B after 112 min (end of test). (b) Map of stress intensity (Von Mises criterion) obtained for test B after 112 min (end of test). In both cases the section of the tank was buffered among the vessel axis in order to show also the inner wall.
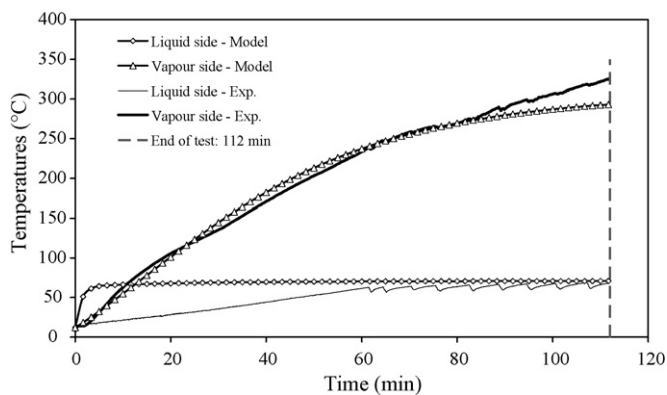
Fig. 12. Comparison of experimental wall temperatures (exp) with FEM simulations (model) for test B. Time since the beginning of the test: 112 min.

Fig. 13. Test B: comparison between coating thickness, wall temperature at the end of test (112 min) and average flame temperature at different positions on the tank shell. Dots are actual temperature measurements, lines represent the estimated temperature trends.

in the simulations (25 mm), assuming an instantaneous reaction between the flame and the coating surface and a sudden growth of coating thickness.

The model solved in each point the basic transient heat balance, expressed in cylindrical coordinates:

$$c\rho \frac{\partial T}{\partial t} = \frac{1}{r}\frac{\partial}{\partial r}\left(k_r \frac{\partial T}{\partial r}\right) + \frac{1}{r^2}\frac{\partial}{\partial \phi}\left(k_\phi \frac{\partial T}{\partial \phi}\right) + \frac{\partial}{\partial z}\left(k_z \frac{\partial T}{\partial z}\right) \quad (1)$$

where T is the temperature, t the time, c the heat capacity, ρ the density, and k the thermal conductivity. For simplicity, the thermal conductivity was supposed uniform among the same material, thus obtaining:

$$c\rho \frac{\partial T}{\partial t} = k\left(\frac{1}{r}\frac{\partial^2 T}{\partial r^2} + \frac{1}{r^2}\frac{\partial^2 T}{\partial \phi^2} + \frac{\partial^2 T}{\partial z^2}\right) \quad (2)$$

A uniform temperature of 12 °C was assumed as the initial temperature for the simulations, on the basis of data from test B. Several boundary conditions are needed to solve Eq. (2). A constant heat load Q_{rad} on the outer surface of tank coating was supposed, due to radiating heat from the external fire, surface emission and convection to/from the atmosphere:

$$k\frac{\partial T}{\partial r}\bigg|_{ext} = Q_{rad} \quad (3)$$

A value of 110 kW/m² was used, derived from standard data available for large diesel pool fires [19,20].
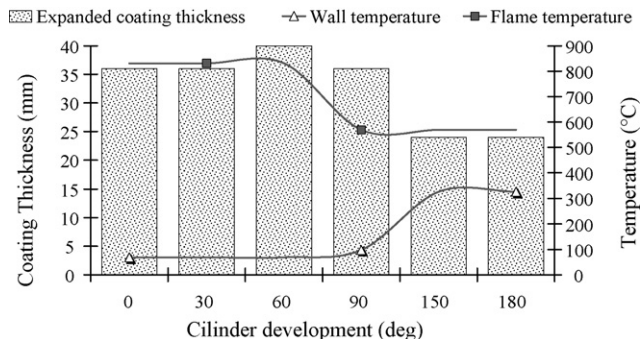
As internal boundary condition, a variable heat load Q_{conv} on the inner tank shell surface, due to the convective heat transfer to the fluid (gas or liquid phase), was supposed:

$$Q_{conv} = h(T - T_B) \quad (4)$$

The value of Q_{conv} depends on wall temperature, and on the bulk fluid temperature (T_B, which can be the liquid or the vapour temperature, depending on the position). The values of the heat transfer coefficients between vessel wall and gas or liquid were derived from a previous study [21], and constant bulk liquid and gas temperatures were assumed, based on the maximum value obtained from the experimental measurements. The parameters used in the thermal simulation are reported in Table 6.

The second step of the modeling was the calculation of the transient stress field as a function of the local temperatures and of the other loads present on the equipment shell. A steady state mechanical analysis was applied in order to reproduce the transient evolution of the stresses on tank walls. Surface loads S were imposed on the inner tank wall, including the variable vapour pres-

Table 7
Absolute and relative error between the measured and the predicted internal wall temperature values

|	Error	
	Absolute (°C)	Relative (%)
Definition	$(T_{mod} - T_{exp})$	$(T_{mod} - T_{exp})/T_{exp} \times 100$
Vapour (maximum)	33	35
Vapour (average)	9	5
Liquid (maximum)	46	278
Liquid (average)	19	64
Liquid, $t > 60$ min (maximum)	11	19
Liquid, $t > 60$ min (average)	7	11

T_{mod}, predicted temperature; T_{exp}, measured temperature.

Fig. 14. (a) Thickness of the coating measured at the end of test B. (b) Thickness of unreacted coating measured at the end of test B after the mechanical abrasive exhausted coating removal. All values are in mm.
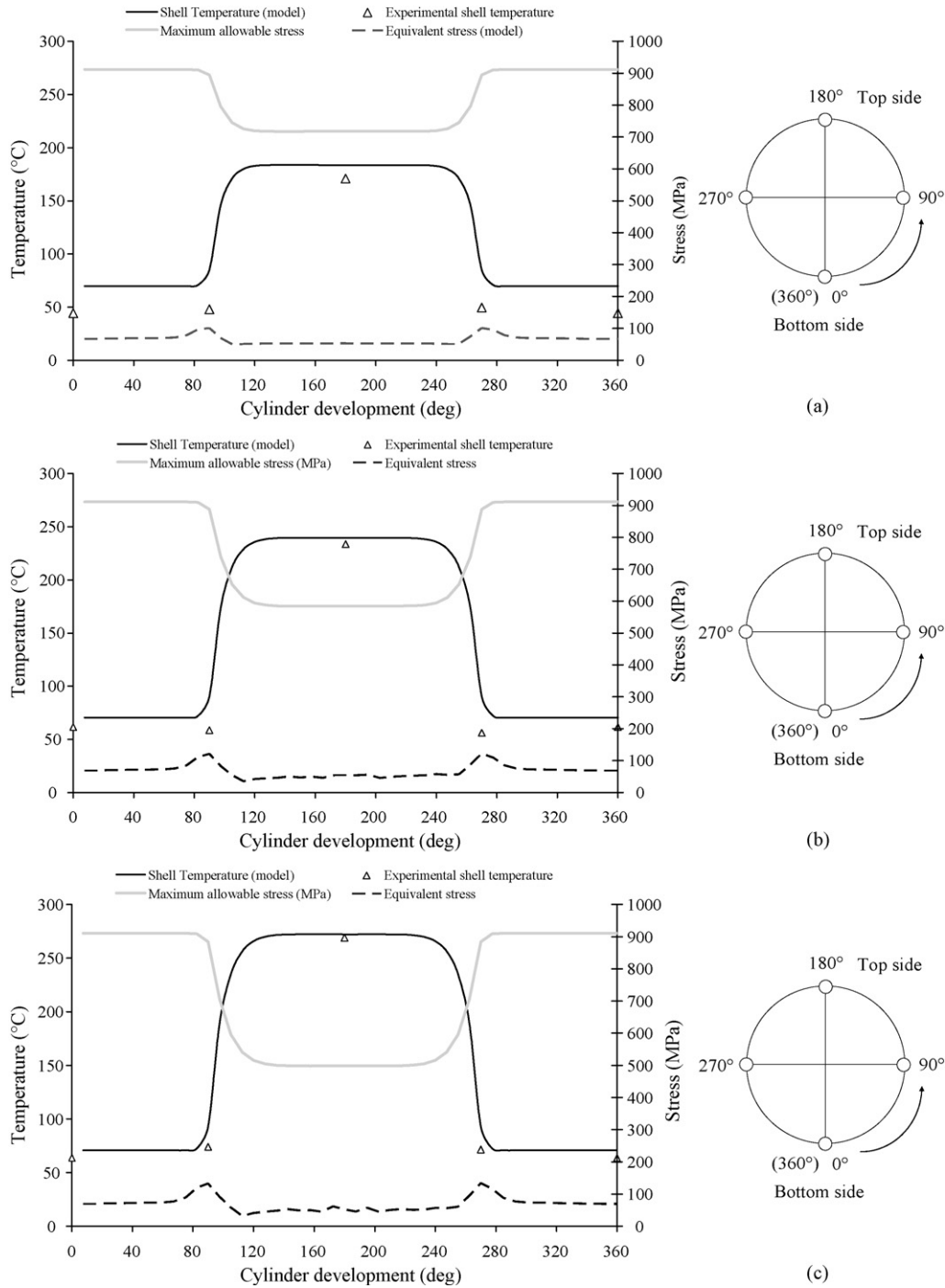
Fig. 15. Test B: temperature (°C), stress intensity (Von Mises criterion) and maximum allowable stress (MPa) of the mean section of the inner tank wall calculated by FEM simulations. Dots: measured values of temperature. Time since test start: (a) 40 min; (b) 60 min; (c) 80 min.

sure p and the hydraulic gradient:

$$S(\phi, t) = p(t) + \rho_l g \frac{D}{2} \sin(\phi) \qquad (5)$$

where ρ_l is the liquid density, g the gravity acceleration (assumed equal to 9.81 m/s^2), D the tank diameter and ϕ the angular coordinate ($\phi = 0$ among the liquid free surface for 50% filling level). As a conservative assumption, the initial filling level was considered in the simulations.

The local temperature values calculated in the thermal simulations were used to evaluate the local stresses, due to thermal

expansion. These are due to the imposed strain ε_T evaluated as follows:

$$\varepsilon_T = \alpha(T_n - T_{n-1}) \qquad (6)$$

where α is the thermal dilatation coefficient, and $n-1$ and n are two consecutive time steps. The software solved the basic mechanical system of equations, in which the vector u of the single nodes displacement is evaluated:

$$Bu = F_M + F_T \qquad (7)$$

where F_M is the vector of mechanical forces (derived in each node from the applied surface pressure S), F_T is the initial force vector, derived from the imposed thermal loads and B is the so called "stiffness matrix", whose elements b_{ij} represent the i-th nodal force when the j-th unitary displacement is applied (with the other displacements equal to zero). The evaluation of the u vector allows the calculation of the deformation of the structure and of the stress distribution [22]. The parameters used in the mechanical simulations are summarized in Table 6.

3.2. Results and discussion

Fig. 11 shows a temperature (a) and stress (b) map obtained in the simulation of test B after 112 min (end of the test). As shown in the figure, the presence of uniform temperature fields is predicted in the lower and in the upper zones of the vessel. The model also predicts the presence of an intermediate region, at vapour–liquid interface, where temperature changes rapidly from values near to those of the liquid to those of the gas. Both these results are in agreement with experimental findings. The temperature trough the insulating coating layer varies from about 930 °C at the outer surface to about 450 °C, near to the inner vessel wall temperature.

Fig. 12 shows a comparison of the experimental and predicted temperature-time plots for the inner side of the vessel wall in the upper and lower zones (respectively in contact with the vapour and with the liquid).

In the case of lower zone temperatures, a sufficient agreement is present after 60 min, at the end of the initial transient. The disagreement among the experimental and model curves in the first part of the test is caused by the simplifying assumptions in the modeling of the liquid temperature, that was assumed constant due to limitations of the commercial code used to implement the FEM approach. Discrepancies between the experimental and the predicted results were analyzed through the definition of reference absolute and relative errors, reported in Table 7. As evident from the table, the model initially overestimates of a factor 3 the liquid temperature. However, this has a negligible influence on overall stresses, due to the low values of liquid temperature at the beginning of the text. As shown in Fig. 12, the error is progressively reduced, and after 60 min the error between the model and the experimental results drastically decreases, falling below 10% (see Table 7). Moreover, the error is always on the safe side.

In the case of the gas temperatures, a good agreement is present among model and experimental data up to about 80 min since the beginning of the test, as shown by Fig. 12 and Table 7. However, in the final part of the test the model under predicts the actual wall temperatures of about 30 °C, although the relative error is limited (about 10%). Again, this error may be caused by model limitations: in particular, constant properties were used for the coating layer, and a uniform behaviour of the protection coating was assumed, without considering the coating consumption due to the charring and combustion process. Both this assumptions seem particularly critical. The use of constant mean properties for the thermal coating was suggested by the supplier and reported in a previous study [21], even if evidences are present that the thermal conductivity of intumescing coatings increases with time of fire exposure [10].

The comparison between the coating thickness and the available temperature measurements, may provide useful information for a preliminary assessment of coating effectiveness. In Fig. 13, the average thickness of the expanded coating in different positions is reported and compared to the maximum recorded external and internal wall temperatures. Data are referred to correspondent spots among the cylinder development, close to the tank support. The figure shows that the expansion of the coating is more pronounced where the flame temperature is higher. In particular, this

is verified in the lower part of the tank, where the highest average flame temperatures are obtained. On the contrary, in the upper part, where the flame temperature is lower, the coating expansion is less pronounced. Fig. 14 reports the measured thickness of the thermal protection layer (a) and the thickness of the unexpanded coating (b) both measured at the end of the test. The figure clearly shows that the expansion of the coating is not homogeneous and that zones of the tank may be present where a less effective thermal protection is provided. Thus, the results thus point out the need for a more thorough understanding of the behaviour and of the performance of intumescing coatings.

With respect to shell stresses, Fig. 11b shows that the stress intensity, calculated by the Von Mises criterion, is higher in correspondence of the vapour–liquid interface (e.g. about 190 MPa), even if the mean wall temperatures are lower than in the upper zone of the vessel, in contact with the vapour phase. This is due to the local thermal stresses generated by the temperature profile of the tank wall between liquid and vapour phases, shown in Fig. 15 at different times. As a matter of fact, a maximum difference of about 200 °C was predicted between the temperatures of the upper zone and of the lower zone of the vessel, well in agreement with the experimental results reported in Fig. 12. This generated an intense local stress field of the wall in the zone of the liquid–vapour interface. These results clearly show the advantages of a detailed analysis, which allows to take into considerations phenomena that are neglected in available simplified criteria based on maximum wall temperatures to assess the possibility of tank failure, e.g. as suggested by and Birk [23] and Lees [24].

Nevertheless, as shown in Fig. 15, the application of the insulating coating was effective in keeping the shell temperatures sufficiently low to allow the steel wall to withstand the stress field generated by the fire, at least for the entire duration of the test (112 min). A FEM simulation carried under the same heat loading conditions indicated that without the thermal protection coating the shell rupture would be expected after about 4 min. These results are confirmed by the experimental tests carried out by Persaud et al. [25] on 4 m^3 unprotected tanks, that reported the tank failure after 4–5 min in full engulfment conditions.

4. Conclusions

Two large-scale diesel pool fire engulfment tests were carried out on LPG tanks protected with intumescing coatings. The tests were performed following a specifically defined test protocol to enhance reproducibility. The geometrical characteristics of the test tanks were selected in order to obtain shell stresses similar to those present in full-size road tankers complying to ADR standards. The results of the fire tests evidenced that the intumescing coating was effective in the protection of the tanks, consistently increasing the expected time to failure. However, both the finite element simulation of test results and the analysis of the thermal protection coating after the test point out that the actual behaviour of intumescing coatings needs to be further investigated to fully understand the effectiveness and reliability of these materials, and to optimize the design of thermal protections. Nevertheless, the preliminary data obtained, indicating an enhanced fire resistance of the protected tanks, suggest that the introduction of fire protection coatings may be a viable route to improve the safety of the LPG distribution chain.

References

[1] M. Molag, Product-chain-analysis ammonia, chlorine and LPG, phase 1 technical, components, economical and external safety aspects in the chain (in Dutch), report R2003/205, Netherlands Organisation for Applied Scientific Research – TNO, Apeldoorn, 2003.

[2] D. Kielec, A.M. Birk, Analysis of tank deformation from fire induced ruptures and BLEVEs of 400 L propane tanks, ASME J. Press. Technol. 119 (3) (1997) 365–373.

[3] B. Droste, W. Schoen, Full scale fire tests with unprotected and thermal insulated LPG storage tanks, J. Hazard. Mater. 20 (1988) 41–53.

[4] W. Townsend, C.E. Anderson, J. Zook, G. Cowgill, Comparison of thermally coated and uninsulated rail tank-cars filled with LPG subjected to a fire environment, report FRA-OR&D 75-32, US Department of Transportation – DOT, 1974.

[5] V. Cozzani, G. Gubinelli, E. Salzano, Escalation thresholds in the assessment of domino accidental events, J. Hazard. Mater. 129 (1–3) (2006) 1–21.

[6] D.F. Bagster, R.M. Pitblado, The estimation of domino incident frequencies: an approach, Process Saf. Environ. 69b (1991) 195–199.

[7] F.I. Khan, S.A. Abbasi, Models for domino effect analysis in chemical process industries, Process Saf. Prog. 17 (2) (1998) 107–123.

[8] M. Molag, A. Kruithof, BLEVE prevention of a LPG tank vehicle or a LPG tank wagon, report R2005/364, Netherlands Organisation for Applied Scientific Research – TNO, Apeldoorn, 2005.

[9] International Carriage of Dangerous Goods by Rail (RID) and by Road (ADR) Safety Committee, document TRANS/GE.15/AC.1/R.79 (OCTI/RID/GT-III/43), Brussels, 1980.

[10] J.M. Faucher, D. Giquel, R. Guillemet, J. Kruppa, Y. Le Botlan, Y. Le Duff, H. Londiche, C. Mahier, I. Oghia, J.L. Py, P. Wiedemann, Fire protection study on fire proofing tanks containing pressurized combustible liquefied gases, GEIE (Groupement Europèen d'Intèret Economico) Paris, GASAFE program report, Paris, 1993.

[11] UN Economic Commission for Europe, Regulation No. 67 Addendum 66 to the Agreement concerning the adoption of uniform conditions of approval and reciprocal recognition of approval for motor vehicle equipment and parts, done at Geneva on 20 march 1958, revision 2 including the amendments entered into force on 16 October 1995 Revision 1, 21 January 2000 (E/ECE/TRANS/505, rev.1/add.66/rev.1), Geneva, 2000.

[12] UN Economic Commission for Europe, Proposal for draft Supplement 5 to the 01 series of amendments to regulation No. 67 (TRANS/WP.29/2004/66) and corrigendum 1, Geneva, 2004.

[13] The European Parliament and the Council of the European Union, Directive 97/23/EC on the approximation of the laws of the Member States concerning pressure equipment, Brussels, 1997.

[14] A.M. Birk, D. Poirier, C. Davison, On the response of 500 gal propane tanks to a 25% engulfing fire, J. Hazard. Mater. 19 (6) (2006) 527–541.

[15] Steel Construction Institute, Availability and properties of passive and active fire protection systems, OTI 92 607, Health and Safety Executive, London, 1992.

[16] H.G. Fisher, H.S. Forrest, S.S. Grossel, J.E. Huff, A.R. Muller, J.A. Noronha, D.A. Shaw, B.J. Tilley, Emergency Relief System Design Using DIERS Technology, The Design Institute for Emergency Relief Systems (DIERS) Project Manual, American Institute of Chemical Engineers, New York, 1992.

[17] C.M. Sheppard, DIERS churn-turbulent disengagement correlation extended to horizontal cylinders and spheres, J. Loss Prev. Process Ind. 6 (3) (1993) 177–182.

[18] C.M. Sheppard, DIERS bubbly disengagement correlation extended to horizontal cylinders and spheres, J. Loss Prev. Process Ind. 7 (1) (1994) 3–5.

[19] L.T. Cowley, A.D. Johnson, Oil and gas fires – characteristics and impact, OTI 92 596, Health and Safety Executive – HSE, London, 1992.

[20] T.A. Roberts, I. Buckland, L.C. Shirvill, B.J. Lowesmith, P. Salater, Design and protection of pressure systems to withstand severe fires, Proc. Saf. Environ. Prot. 82 (B2) (2004) 89–96.

[21] M. Molag, J.E.A. Reinders, S.J. Elbers, Onderzoek naar de effectiviteit van maatregelen ter voorkoming van een warme BLEVE van een autogas tankauto (in Dutch), report 2006-A-R0307/B, Netherlands Organisation for Applied Scientific Research – TNO, Apeldoorn, 2006.

[22] ANSYS INC., ANSYS^{TM} user guide, v.11, 2007.

[23] A.M. Birk, Scale effects with fire exposure of pressure-liquefied gas tanks, J. Loss. Prev. Process Ind. 8 (5) (1995) 275–290.

[24] F.P. Lees, Loss Prevention in the Process Industries, second ed., Butterworth-Heinemann, Oxford, 1996.

[25] M.A. Persaud, C.J. Butler, T.A. Roberts, L.C. Shirvill, S. Wright, Heat-up and failure of liquefied petroleum gas storage vessel exposed to a jet-fire, in: Proceedings of 10th International Symposium on Loss Prevention in the Process Industries, Stockholm, 2001, pp. 1069–1106.